

Document downloaded from:

<http://hdl.handle.net/10251/123497>

This paper must be cited as:

Galindo, J.; Climent, H.; Varnier, O.; Patil, CY. (2018). Effect of boosting system architecture and thermomechanical limits on diesel engine performance: Part I -Steady-state operation. *International Journal of Engine Research*. 19(8):854-872.
<https://doi.org/10.1177/1468087417731654>



The final publication is available at

<http://doi.org/10.1177/1468087417731654>

Copyright SAGE Publications

Additional Information

Effect of boosting system architecture and thermomechanical limits on diesel engine performance. Part-I: Steady State Operation

Jose Galindo, Hector Climent, Olivier Varnier[†], Chaitanaya Patil*
CMT-Motores Térmicos, Universitat Politècnica de València, Valencia 46022, Spain.,

[†]Jaguar Land Rover Ltd., UK.,

*e-mail : chpa7@mot.upv.es

07/11/2016

Abstract

Internal combustion engines developments are focused on efficiency optimization and emission reduction. To achieve these, downsized or downspeeded engines are required which can reduce fuel consumption and CO₂ emission. However, these technologies ask for efficient charging system. This paper consists of study of different boosting architectures (single stage and two stage) with combination of different charging system like superchargers, e-boosters etc. A parametric study is carried out with a 0D engine model to analyze and compare different architectures on same base engine. The impact of thermomechanical limits, turbo sizes and other engine development options characterizations are proposed to improve Fuel consumption, maximum power and performance of the downsized/downspeeded diesel engines.

1 Introduction

The potential of new emerging turbocharging architectures to enhance the performance of downsized and down speeded engines has taken a crucial part. Upcoming new emissions test cycles are much more demanding with high EGR rates and transients. Moreover, turbocharger size, thermomechanical limits have also important consequences on engine performance and their impact have to be characterized to quantify possible benefits modifying their values. This

23 paper focuses on a comprehensive study with the 0D engine model to respond to these specific
24 objectives. A sophisticated model that includes a 0D phenomenological combustion model
25 (combustion process) (*I*) and a 0D filling and emptying model (multi-cylinders and manifolds)
26 was then developed to achieve the model complexity required by this study.

27 This study is divided into two papers, first part consist of the analysis of the engine and
28 boosting systems performance under steady-state operations along with the hypotheses that
29 have been assumed accordingly. (The results obtained with the main turbocharger will thus be
30 reported before those obtained in two-stage operations). Following the future needs in charger
31 development, the operating ranges required by downsized-down speeded engines will be con-
32 fronted to conservative supercharger, compressor and turbines characteristics maps. At last, the
33 transient aspects will be considered with an analysis of the boosting architectures performance
34 on different downsized engines during cold transient test cycles.

35 **2 Modelling and Methodology**

36 The OD model has been created with Matlab considering several degrees of engine downsizing.
37 So the engine scaling process based on a similarity approach is carried out. Finally, the other
38 hypotheses made on the input data relating to the gas path elements, injections settings and EGR
39 systems. Three passenger car Diesel engines have been involved in the characteri- zation and
40 validation work. The first two engines (referred as Engine A and B) have been designed by the
41 French manufacturer PSA under the Euro IV emissions regulations, while the third one (Engine
42 C) has been more recently designed by Renault and respect the Euro V regulations.

43 **3 Boosting Architectures**

44 It has been highlighted the most promising boosting systems to increase the performance of
45 automotive downsized-downspeeded engines are sequential serial two-stage turbocharging, me-

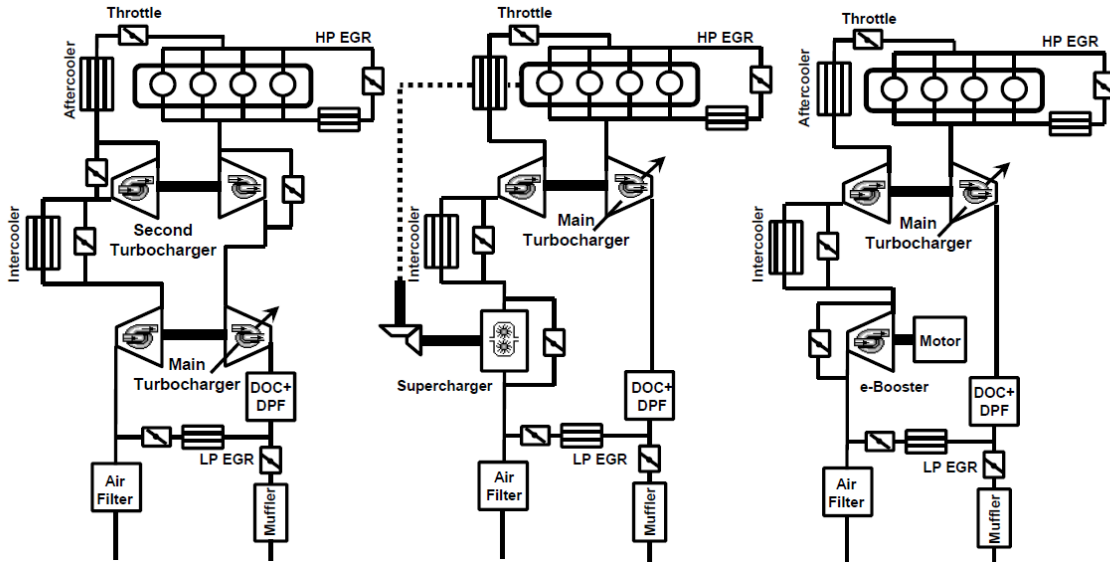


Figure 1: Two-Stage Boosting architectures

46 chanical auxiliary supercharging and electric booster. (17) These architectures have thus been
 47 analyzed in this chapter and a schematic of each one of them can be observed in figure 1. All
 48 architectures are composed of a main turbocharger fitted with a variable geometry turbine, a HP
 49 and LP EGR circuit equipped with their corresponding valves and cooler, an intake throttle to
 50 forced HP EGR mass flows when necessary, an air filter, an after treatment system and a muffler.
 51 To cool the intake gas, an aftercooler is positioned before the intake manifold. An additional
 52 intercooler can also be employed between both stages to perform an extra cooling through the
 53 control of a bypass valve. In the serial two-stage turbocharging system, the second turbocharger
 54 is fitted in the HP stage with a fixed geometry turbine while in the other systems, the mechan-
 55 ical supercharger and the e-Booster are placed in the LP stage. Finally in each configuration
 56 a bypass valve is arranged around the second charger to avoid parasitic losses in single-stage
 57 operations (sequential mode).

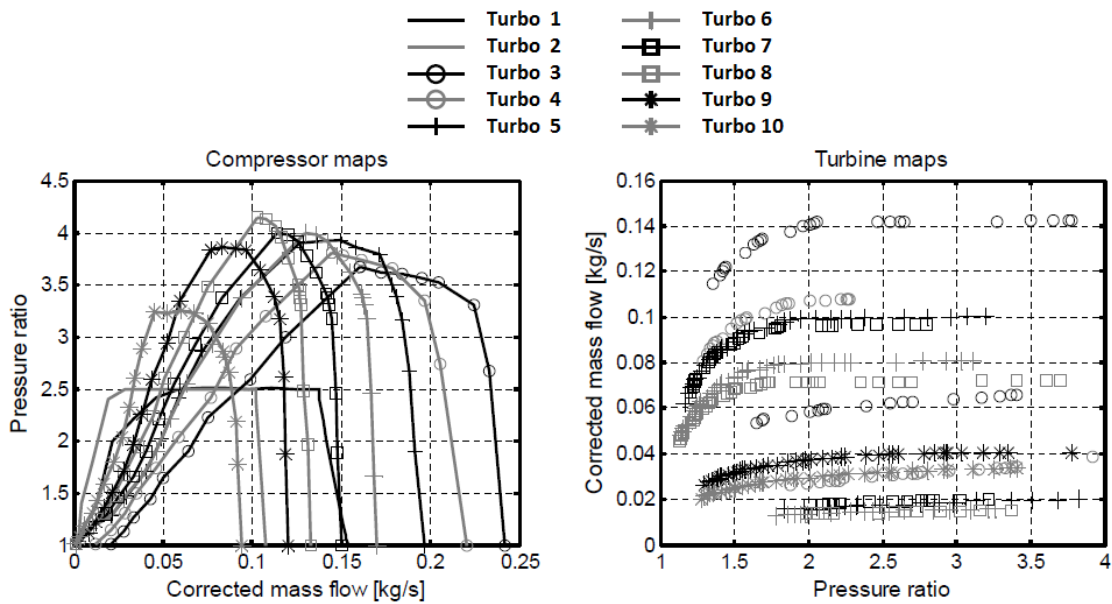


Figure 2: HTT turbocharger family and small Eatons superchargers map

58 3.1 Turbochargers

59 The information relating to the turbochargers comes from characteristics maps measured in
 60 turbocharger test benches (?). These data correspond to specific compressor and turbine designs
 61 which can be optimized for each application to achieve particular objectives. In the automotive
 62 market, a wide range of turbocharger designs are present and no map generalization can be
 63 made to perform global parametric studies. As shown in figure 2 where compressors and
 64 superchargers operating ranges have been plotted, the maps from an entire turbocharger family
 65 can give information about the actual technological limits. But both surge line and over speed
 66 limits (respectively right limit and left limit of the compressor maps) are too dependent of the
 67 installation and measuring methods (8) (9) (16) to be assumed as strict limiting factor in the
 68 calculations.

69 Efficiencies are also strongly dependent of wheels designs and important variations can be
 70 observed between different turbochargers with similar operating ranges. That is why in this

		Main Turbocharger		Second Stage	
		Compressor	Turbine	Compressor	Turbine
Single-Stage	State-of-art	70	65	-	-
	Hypothesis	80	75	-	-
Two-Stage Turbocharger	State-of-art	70	65	67	65
	Hypothesis	80	75	77	75
Two-Stage Supercharger	State-of-art	70	65	65	-
	Hypothesis	80	75	75	-
Two-Stage eBooster	State-of-art	70	65	67	-
	Hypothesis	80	75	77	-

Figure 3: Charger efficiencies used in the steady state calculations

71 study, particular characteristic maps have not been used in the steady-state calculations and
72 an energetic approach has been preferred. This energetic approach avoids design influences
73 assuming infinitely large turbocharger operating ranges and making some hypotheses on the
74 efficiencies. The charger efficiencies used in steady state calculations are showed in figure 3

75 **3.2 Gas Path Elements**

76 Pressure losses in the intake and exhaust lines elements have important impacts on engine and
77 boosting architecture performance. Their characteristics are mainly dependent of mass flow rate
78 and component design. The selection of the engine elements is specific to each application and
79 responds to a delicate balance between pressure drops, packaging constraint, efficiency to fulfill
80 the component function, cost, etc. . . So, an energetic approach has also been considered for
81 the engine components to generalize their pressure losses characteristics to the different engine
82 displacements and rated power levels (maximum mass flow)

83 Pressure losses measured under full load conditions in the air filter, aftercooler, and muffler
84 and after treatment system of Engine C (mentioned in methodology) are shown in table 4. As
85 similar drops have also been measured on the engines A and B, especially for the aftercooler

Engine speed	Air filter	Aftercooler	Muffler	DOC+DPF reference	DOC+DPF large capacity
1000 rpm	11	10	10	38	19
1250 rpm	13	16	18	74	37
3000 rpm	73	72	117	468	234
3500 rpm	98	101	160	644	322

Figure 4: Pressure losses (mbar) in gas path elements under full load conditions

86 and muffler, the same data have been considered independently of the mass flow rate. This
87 hypothesis amounts to scaling the pressure losses characteristics for each application in order
88 to maintain the same component influences in the simulations. A picture of this hypothesis is
89 given in figure 5 where it can be seen how the reference pressure losses characteristic is adapted
90 to the considered maximum gas mass flow.

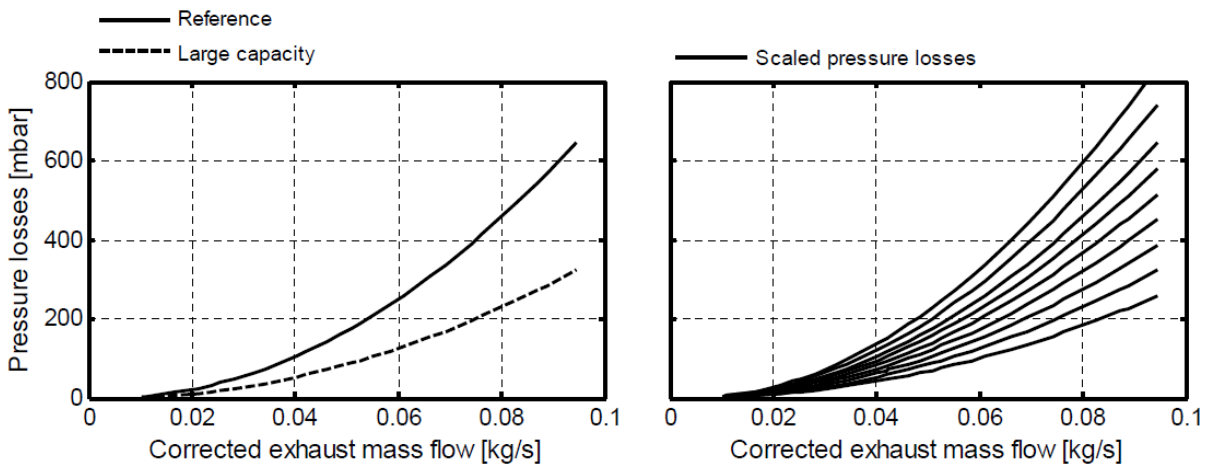


Figure 5: scaled pressure loss characteristics in aftertreatment system

91 The after treatment system is the engine component that involves the higher pressure drops.
92 To analyze the performance sensitivity of its design, a large capacity system producing only
93 half losses has also been considered. For the charge air coolers, the same pressure losses char-
94 acteristics have been employed for the intercooler and aftercooler and NTU models have been

95 replaced by ideal cooling efficiencies (external cooling fluid temperatures of 35°C).

96 **3.3 Injection Setting**

97 To limit the number of parameters, the injection process has been reduced to a unique main
98 injection without any pre- or post-injections. The injection timings have been optimized to
99 maximize the IMEP (minimum specific fuel consumption) or to respect the maximum allowable
100 cylinder pressure. At 1000 rpm and 1250 rpm, the relative fuel-to-air ratio has been fixed to 0.9.
101 This value represents a typical maximum fuel-to-air ratio allowed by smoke limiters. While at
102 3000 rpm and 3500 rpm, a fuel-to-air ratio of 0.7 has been retained to limit exhaust manifold
103 temperatures. This lower fuel-to-air ratio obviously imposes a higher demand on the boosting
104 system. That is why its value has been progressively increased up to 0.9 when turbine inlet
105 pressure or compressor outlet temperature becomes a limiting factor.

106 **3.4 EGR System**

107 Low Pressure and High Pressure EGR systems have been analyzed under three different EGR
108 rates: 0% (without EGR), 15% (Euro VII objectives) and 30% (strong EGR constraint). In
109 the coolers, ideal efficiencies have been employed with external cooling fluid temperatures of
110 90°C. Their pressure losses have been fixed in the calculations at 3 mbar at 1250 rpm, 18 mbar
111 at 3000 rpm and 25 mbar at 3500 rpm. EGR performance has not been considered at 1000 rpm
112 as no emissions test cycle requires EGR under full load at that speed. For the other gas path
113 components, two hypotheses have been assumed on their pressure losses characteristics. On
114 the one hand, the same pressure drops have been used between the three different EGR rates
115 scaling the elements characteristics for each running operation. In that way, as LP EGR involves
116 higher gas mass flows in the intake/exhaust lines, bigger charge air coolers and after treatment
117 system effective sections are considered for LP EGR operations. On the other hand, the same

118 pressure losses characteristics have been employed under LP and HP EGR rates scaling the
119 characteristics for the LP EGR mode. In that case, the same elements are considered between
120 both modes and pressure drops in charge air coolers as after treatment system result lower in
121 the HP EGR mode. In the following section, this second hypothesis is labeled HP EGR low dP.

122 **4 Steady State Results**

123 As the main objective of these simulations was to characterize the boosting system and the
124 thermomechanical limits affecting the maximum reachable brake power. Hence The operating
125 conditions have been defined as a function of brake power objectives increasing brake power
126 until reaching one of the thermomechanical limits. With the energetic approach, the different
127 engine components are directly matched to the considered brake power level so that the obtained
128 results correspond to the optimized configurations.

129 To compare the different architectures and to analyze the influences of the considered de-
130 sign factors, the Brake Specific Fuel Consumption (BSFC) has been retained. Generally under
131 full load conditions, BSFC is not so important because the current passenger cars emission test
132 cycles dont include these running conditions. But this parameter becomes relevant for future
133 engine development as the new emission test cycles integrate more and more highly loaded op-
134 erations. Furthermore here, BSFC has been selected to quantify in each study the overall system
135 efficiency taking into account not only the engine or the boosting architecture performance but
136 also all the systems interactions. The BSFC allows therefore to evaluate the impact of each
137 parameter from a global point of view such as the brake thermal efficiency.

138 For the thermomechanical limits, two levels of maximum compressor outlet temperature
139 have been defined, one at 190°C and one at 210°C. The first level corresponds to the old part
140 in turbocharger and intake line development, while the second represents the maximum allow-
141 able working temperature for cast aluminum alloy compressor wheels. This second level does

Engine speed	State-of-art	Hypothesis
1000 rpm	130 bar	150 bar
1250 rpm	150 bar	180 bar
3000 rpm	170 bar	190 bar
3500 rpm	170 bar	190 bar

Figure 6: Maximum incylinder pressure used in the simulations

not involve major modifications in compressor wheel design but requires advanced plastic materials for the intake piping. Although turbine inlet pressures have also been limited at 4.5 bar, maximum compressor outlet temperatures have always been a more restrictive factor in the calculations. Here, exhaust temperatures have not been constrained in order to define new maximum temperature requirements.

4.1 Effects of Maximum Allowed In-cylinder Pressure

For maximum in-cylinder pressures, two levels have been analyzed: one corresponding to the past in engine development and one considering future thermomechanical limits evolutions (19) (13). These limits, which depend on engine speed, are defined to ensure that oscillating gas force loads do not exceed the material fatigue strength in bearing and cylinder head top desk areas. The considered values are shown in table 6 while the performance results are plotted in figure 7

As it can be observed in figure 7, the BSFC presents a trend that firstly decreases and then increases as a function of brake power level. This trend is explained by both combustion velocity and injection timings. In fact, increasing the brake power level increases the charge density in the combustion chamber accelerating the RoHR and improving the combustion efficiency. However, when the maximum in-cylinder pressure is reached, injection timings are retarded and combustion efficiency decreases.

A higher maximum in-cylinder pressure moves therefore the point of minimum BSFC to higher BMEP and reduces the BSFC at high BMEP. At low speeds with moderate BMEP ob-

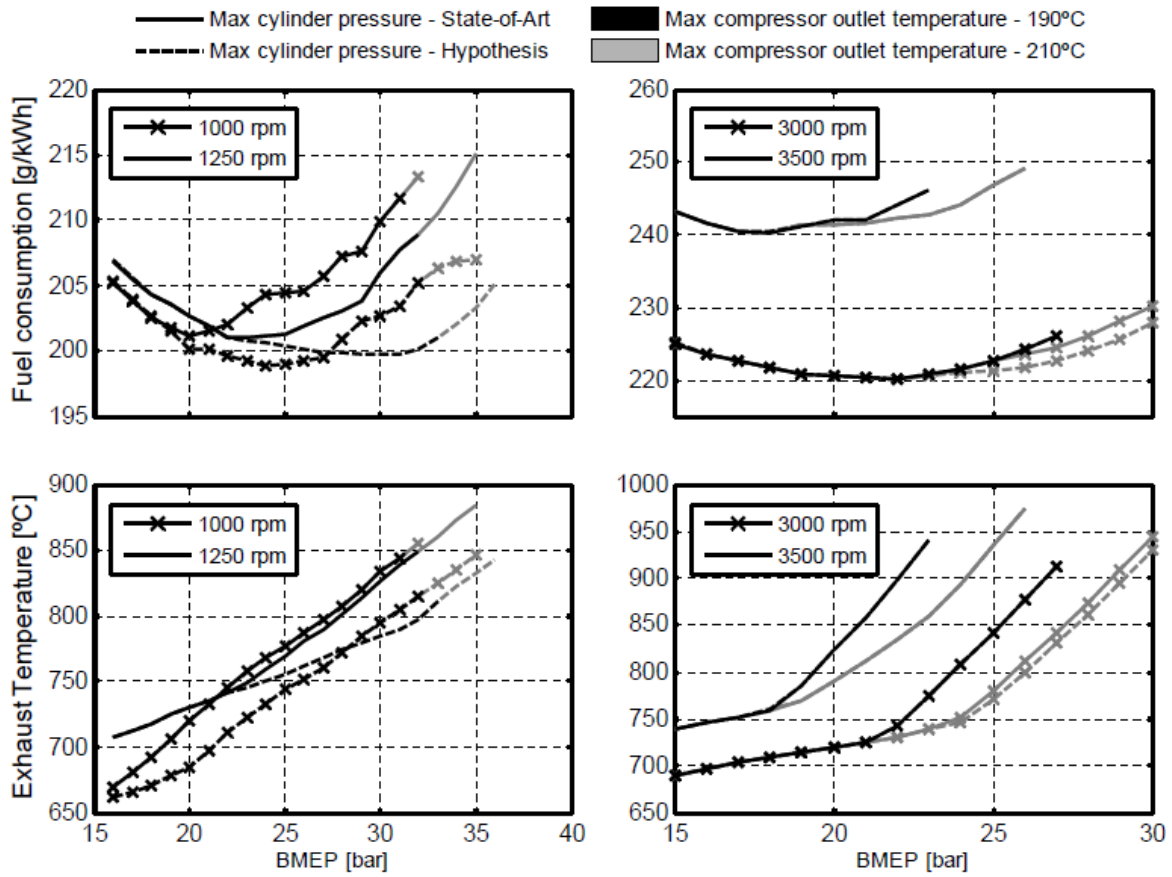


Figure 7: Impact of maximum in-cylinder pressure and maximum compressor outlet temperature on engine performance as a function of brake power levels

161 jectives (around 20 bar), there are no benefits to increase the actual state-of-art limits. But for
162 strong BMEP objectives (around 30 bar), fuel savings up to 7 g/kWh can be obtained. Exhaust
163 temperatures rise more or less linearly with the brake power level. Increasing the maximum in-
164 cylinder pressure allows also the reduction of the temperature constraints at high BMEP limiting
165 the need to retard injection timings.

166 At 3000 rpm and 3500 rpm, the variation of fuel-to-air ratio is an additional factor affecting
167 the BSFC. The change of trend noticed on the exhaust temperature shows how the fuel-to-air ra-
168 tio is gradually increased to respect the maximum compressor outlet temperatures. A relatively
169 low fuel-to-air ratio requires a higher compression work but reduces the thermal constraint in
170 the exhaust. It also increases the charge density and oxygen concentration in the combustion
171 chamber. As already explained a higher charge density can improve or deteriorate the BSFC,
172 while a higher oxygen concentration always increases the combustion velocity and the corre-
173 sponding combustion efficiency. The impact of lower fuel-to-air ratio on BSFC is therefore a
174 balance between boosting systems losses and combustion benefits which mainly depends on
175 the in-cylinder pressure limit. This balance is generally positive until the injection timings need
176 to be delayed. At 3500 rpm, the in-cylinder pressures do not reach the state-of-art pressure
177 limits. So, the fuel consumption increases from the moment when fuel-to-air ratio rises. The
178 same effect is observed at 3000 rpm with the 190°C limit at the compressor outlet. With the
179 210°C limit, the fuel consumption increases before modifying the fuel-to-air ratio as the higher
180 charge density requires some injection timings delays. Nonetheless, these injection timings
181 delays are relatively small and generate only resultant fuel penalties of 2 g/kWh. From these
182 considerations, at 3000 rpm and 3500 rpm the differences in BSFC are therefore mainly ex-
183 plained by fuel-to-air ratio variations and the small benefits observed at 3000 rpm do not justify
184 an increase of the current state-of-art in-cylinder pressure limits at rated speeds. In terms of
185 maximum BMEP, the maximum allowable compressor outlet temperature always limits cylin-

186 der charge densities before exceeding the maximum in-cylinder pressure at the end of the
187 compression stroke. Extending the thermal limit from 190°C to 210°C allows to increase the
188 maximum BMEP of around 3 bar at rated speeds and between 1 bar and 3 bar at low speeds.
189 At low speeds, similar benefits are also obtained increasing the maximum in-cylinder pressures
190 due to higher combustion efficiencies (more centered injection timings). Maximum in-cylinder
191 pressures appear therefore as indirect limiting factors. These results are obviously dependent
192 of the cylinder compression ratio. If a higher value is retained, the impacts observed on the
193 BSFC will be more marked but the main trends will remain and the curves will be only shifted
194 to lower BMEP. Finally comparing running operations performed at 3000 rpm and 3500 rpm,
195 the effectiveness of the downspeeding technique to reduce fuel consumption can be noticed
196 with differences up to 20 g/kWh between both considered rated speeds. Exhaust temperature
197 constraints stay as for them relatively constant.

198 **4.2 Effects of Exhaust Back Pressure**

199 The influences of engine components pressure losses characteristics on engine and boosting
200 system performance are shown in figure 8. Having higher pressure drops, a sensitivity study
201 has been performed on the aftertreatment system considering a reference and a large capacity
202 design as previously described. With both designs, it can be observed that elements pressure
203 characteristics have minor impacts at 1000 rpm and 1250 rpm because gas mass flow as pres-
204 sure drops are relatively small at these speeds. However at high engine speeds, their impacts
205 have important consequences on the BSFC. In fact here it can be noticed how pressure losses
206 differences of 234 mbar and 322 mbar between both designs at 3000 rpm and 3500 rpm offset
207 the BSFC of around 5 g/kWh and 10 g/kWh respectively. In addition, the large capacity design
208 in- creases the maximum reachable BMEP of 1 bar decreasing the exhaust thermal constraints
209 of around 30°C at both rated speeds. The optimization of elements pressure characteristics is

210 therefore fundamental to improve in the medium to high speed range the fuel consumption of
 211 downsized-downspeeded engines.

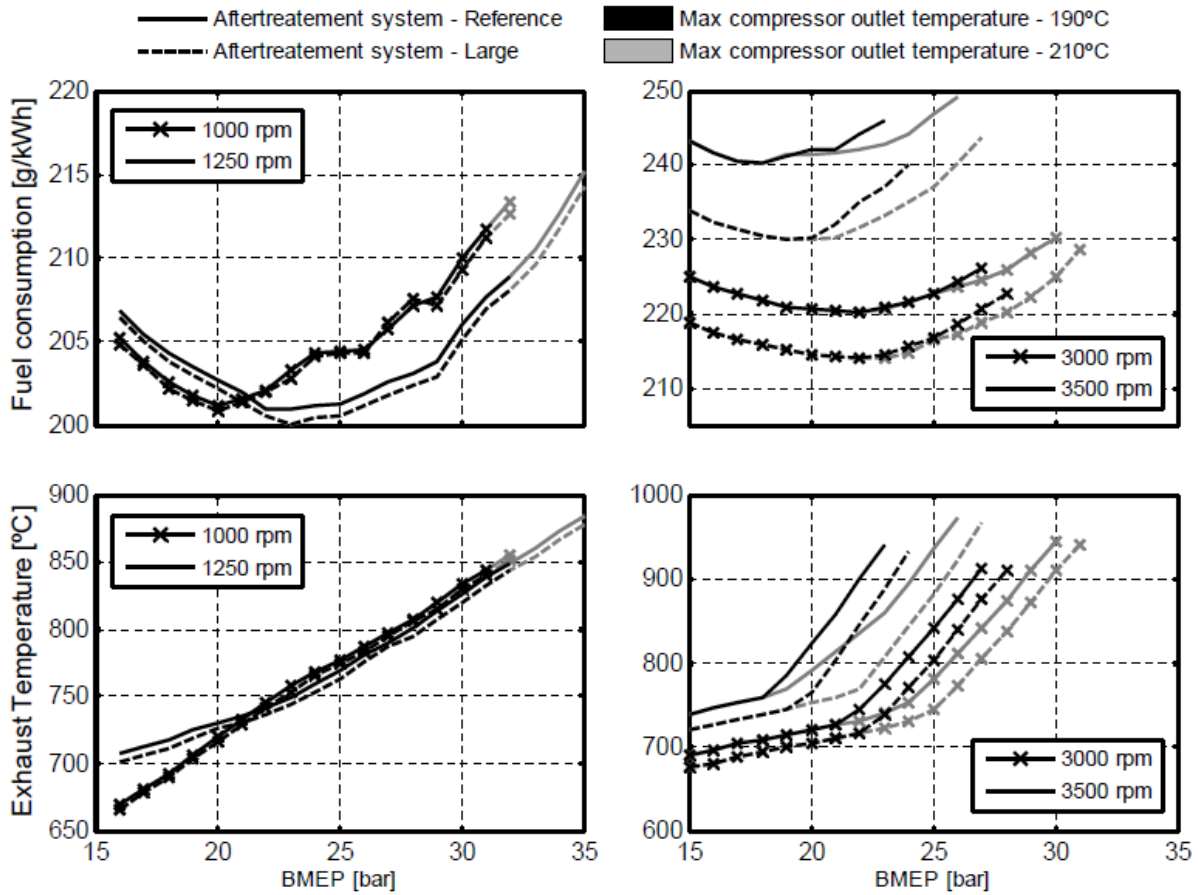


Figure 8: Impact of pressure drops across the aftertreatment system and maximum compressor outlet temperature on engine performance as a function of brake power levels.

212 4.3 Effect of Turbocharger Efficiency

213 For the influences of turbocharger efficiencies on engine and boosting system performance,
 214 different hypotheses have been assumed to fix state-of-art levels before considering variations
 215 of 10 points on both compressor and turbine efficiencies. As it can be observed in figure
 216 9, these important efficiency variations have limited consequences on the BSFC at low speeds

217 reaching fuel savings of only 2-3 g/kWh at 1000 rpm and 1250 rpm. However at rated speeds,
 218 their impacts are much more significant achieving BSFC reductions of around 5 g/kWh and 10
 219 g/kWh at 3000 rpm and 3500 rpm respectively. These reductions are similar to those obtained
 220 with the large capacity after treatment system. That means, optimizing the elements pressure
 221 characteristics can bring the same BSFC benefits as increasing by 10 points the turbocharger
 222 efficiencies. In terms of maximum BMEP, compressor outlet temperatures are highly dependent
 223 of turbocharger efficiencies and variations of 10 points allow to increase the maximum BMEP
 224 of around 3-4 bar in the whole engine speed range.

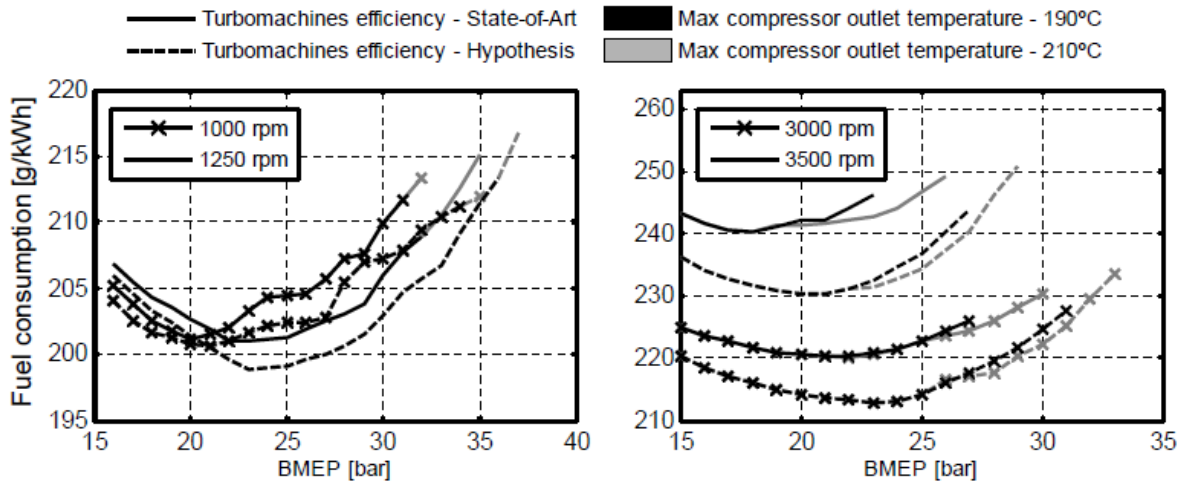


Figure 9: Impact of turbocharger efficiencies and maximum compressor outlet temperature on engine performance as a function of brake power levels.

225 These results also demonstrate that the conclusions obtained with this energetic approach
 226 can be generalized to similar downsized-downspeeded engines. In fact, efficiency hypotheses
 227 have been established with a turbocharger size corresponding to a 2.3l engine. But it has been
 228 shown maximum efficiency variations do not exceed 3 points for the compressor and 5 points for
 229 the tur- bine when smaller turbochargers and smaller engine displacements are considered (1.2l-
 230 1.6l engines). These efficiency variations are relatively limited when compared to the variations

231 performed in the sensitivity study. As efficiency variations mainly offset the performance results
232 keeping identical trends, the same conclusions can be easily extrapolated to other turbocharger
233 efficiencies and to other engine displacements.

234 **4.4 Synthesis of Thermal Constraint**

235 In order to analyze how the thermal constraints limit the engine performance, the maximum
236 reachable BMEP obtained in the previous sensitivity studies have been plotted in figure 10 with
237 several levels of maximum exhaust temperature. As the simulations are not limited by tur-
238 bocharger operating ranges, it can be noticed that maximum BMEP are higher at low speeds
239 than at rated speeds. This is mainly explained by lower gas path pressure losses and lower
240 friction plus auxiliaries mechanical losses suffered at reduced speeds. Between both considered
241 rated speeds, the higher losses suffered at 3500 rpm offset the brake power benefits implied by a
242 higher speed and both downspeeding levels achieve similar maximum engine powers. Regard-
243 ing the different component optimization scenarios, turbocharger efficiencies and maximum
244 in-cylinder pressures involve the major BMEP variations at low speeds. While at high speeds,
245 the major BMEP variations are produced by turbocharger efficiencies and element pressure
246 characteristics.

247 These results have been obtained limiting directly the maximum outlet compressor tem-
248 perature in the calculations. Taking into consideration the exhaust thermal constraints, it can
249 be seen the maximum exhaust temperature is much more restrictive than the maximum outlet
250 compressor temperature. In fact, the allowable exhaust temperature must be higher than 850°C
251 at low speeds and higher than 950°C at rated speeds so that the maximum outlet compressor
252 temperature becomes the limiting factor. A high exhaust temperature limit is therefore a fun-
253 damental requirement to increase the performance of downsized-downspeeded engines. Due to
254 torque limitations in vehicle trans- mission, maximum BMEP objectives are generally constant

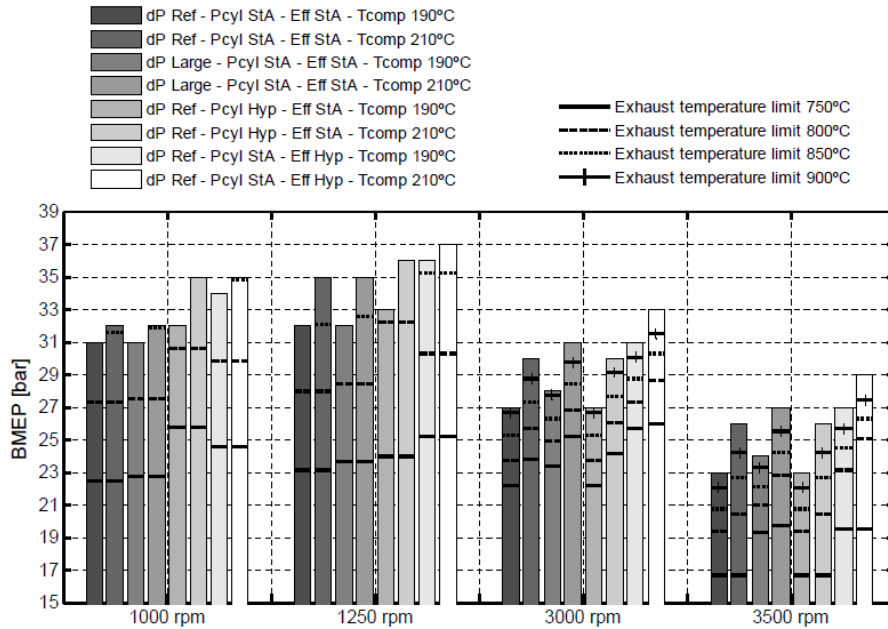


Figure 10: Influences of thermal constraints on maximum reachable BMEP for different component optimization scenarios.

255 between 1250 rpm and rated speed. Analyzing the results at iso-BMEP objectives, it can be
 256 noticed the exhaust temperatures are higher at rated speeds than at 1250 rpm despite the lower
 257 fuel-to-air ratio. The rated power represents thus the most critical running operation and exhaust
 258 temperature limitations must be rated at that point. Nowadays, exhaust temperature limitations
 259 vary between 750°C and 850°C according to the load duty cycle of each application. But ex-
 260 haust manifolds and turbochargers able to withstand temperatures higher than 1050°C have
 261 already been developed for passenger car gasoline engines (20). Considering the exhaust con-
 262 straints shown in figure 10, materials and turbocharger technologies used on gasoline engines
 263 are thus necessary to develop highly-rated Diesel downsized-downspeeded engines.

264 **4.5 Effect of EGR Level**

265 EGR requirements imposed by new emission test cycles have important consequences on the
266 engine and boosting system performance. To analyze these consequences, a first sensitivity
267 study has been performed on the EGR rate provided by the LP EGR circuit. The previous pa-
268 rameters (engine components pressure characteristics, turbocharger efficiencies and maximum
269 in- cylinder pressure) have been maintained at their conservative or reference values. Low Pres-
270 sure EGR has an impact on the combustion process, the turbocharger work and the gas path
271 pressure drops. Here, with the hypotheses assumed on the pressure losses characteristics, the
272 engine components are directly matched to the different LP EGR rates and gas mass flows. So
273 the components pressures losses do not have any influence in this first EGR sensitivity study.
274 Besides with the pressure drops retained for the air filter and muffler, the use of the second
275 LP EGR valve placed at the muffler inlet has not been required in the calculations. For the
276 combustion process, EGR increases the density in the combustion chamber but reduces signif-
277 icantly the oxygen concentration and the resultant combustion velocity. Combustion efficiency
278 and fuel consumption are thus deteriorated with EGR. However, a slower combustion velocity
279 decreases the in-cylinder pressure and requires lower injection delays to respect the in-cylinder
280 pressure limitations. In that case, the more centered combustion obtained with EGR can im-
281 prove the fuel consumption. This effect depends obviously on the hypotheses assumed for the
282 injection settings and can be avoided using multi-injection strategies or defining other objec-
283 tives for the injection timings optimization process. For the turbocharger, LP EGR increases
284 the compressor gas mass flow and the required turbocharger work to provide a given boost. LP
285 EGR increases also the gas mass flow passing through the turbine but this higher flow does not
286 offset the higher compression work and turbine expansion ratio increases. Introducing EGR
287 in the cylinders lowers gas temperature during the combustion process and reduces the avail-
288 able energy at the turbine inlet which further in- creases the turbine expansion ratio. LP EGR

289 deteriorates therefore the fuel consumption due to higher engine pressure losses.

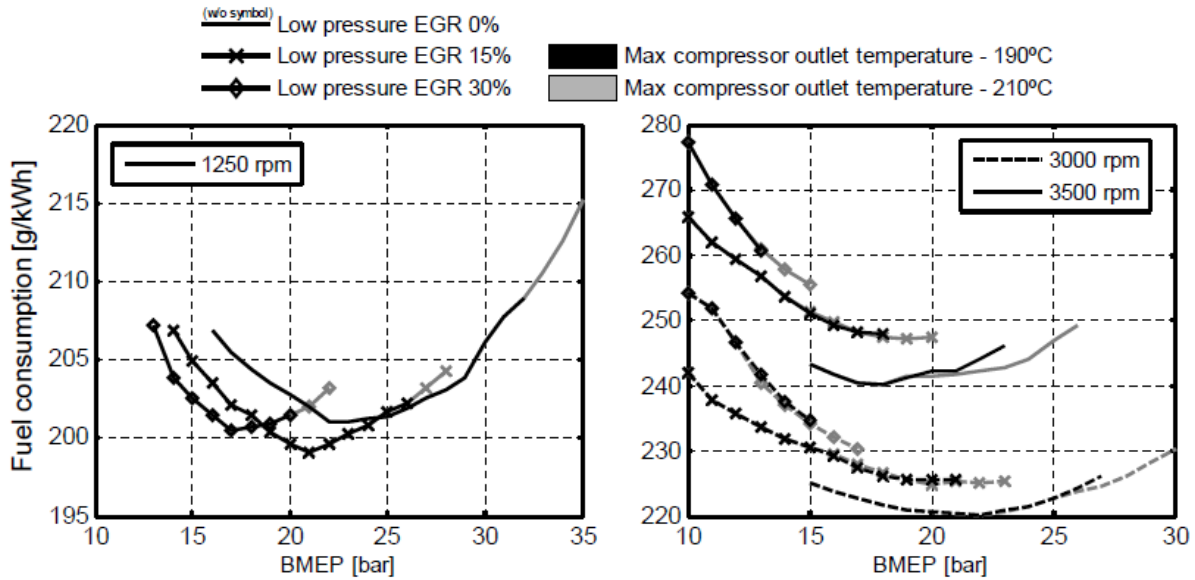


Figure 11: Impact of LP EGR rates and maximum compressor outlet temperature on engine performance as a function of brake power levels.

290 In figure 11, the balance of these different impacts can be observed for various LP EGR rates
 291 (0%, 15% and 30%). At 1250 rpm, the higher cylinder charge densities move the BSFC curves
 292 and the point of minimum fuel consumption to lower BMEP. With a LP EGR rate of 15%,
 293 the lower injection delays allow fuel benefits that largely compensate for the losses involved
 294 by higher turbine expansion ratios and BSFC are improved. With 30%, the combustion bene-
 295 fits just offset the backpressure losses and BSFC are relatively closed to ones obtained without
 296 EGR. In terms of maximum BMEP, even employing an ideal EGR cooler which corresponds to
 297 the most optimistic situation, the maximum compressor outlet temperature strongly limits the
 298 engine performance with decreases of 7 bar and 13 bar under LP EGR rates of 15% and 30%
 299 respectively. In two-stage architectures, these performance falls can be minimized dividing the
 300 compression work between the HP and LP stages and using an intermediate intercooler. But at
 301 low speeds, the main turbocharger has generally no ability to produce significant compression

302 works forcing the boosting architecture operating only with the second charger. In these con-
303 ditions, an intermediate intercooler does not present any potential to maintain or increase the
304 engine performance. At 3000 rpm and 3500 rpm, increasing by 15% the LP EGR rates generates
305 fuel consumption penalties from 5 g/kWh to 10 g/kWh. In fact, the in-cylinder pressure limi-
306 tations have lower influences on the injection timings and the injection strategy does not bring
307 any fuel benefits when working with EGR. The gas mass flows are also relatively important and
308 the backpressure losses generated by higher turbine expansion ratios become significant. For
309 the maximum BMEP, performance reductions from 5 bar to 7 bar can be no- ticed between the
310 different EGR rates. These performance reductions cannot be minimized by an intermediate
311 intercooler because the second charger is generally too small to provide boost at these speeds.

312 **4.6 Effect of EGR Architecture**

313 With these results, a second sensitivity study has been carried out to analyze the impacts of
314 the EGR circuit (High Pressure and Low Pressure) to provide different EGR rates (15% and
315 30%). The main differences between both EGR circuits lie in turbocharger works and intake
316 temperatures. Under LP EGR, turbocharger works are more important due to higher gas mass
317 flows passing through the intake/exhaust lines and intake temperatures are lower thanks to the
318 aftercooler cooling process. Considering ideal aftercooler and EGR coolers, the intake temper-
319 ature variations reach 8°C and 16°C under 15% and 30% EGR respectively. These temperature
320 variations deteriorate the engine breathing process. Higher boosts are therefore necessary under
321 HP EGR to admit the desired gas mass flows into the cylinders. As previously described for the
322 pressure losses characteristics, two hypotheses have been assumed; one considering the same
323 pressure drops between both systems (HP EGR) and one considering the same elements effec-
324 tive sections (HP EGR Low dP). The results of this analysis are shown in figure 12. Having the
325 same trends, the 3500 rpm rated speed operations have not been represented here for the sake

326 of clarity.

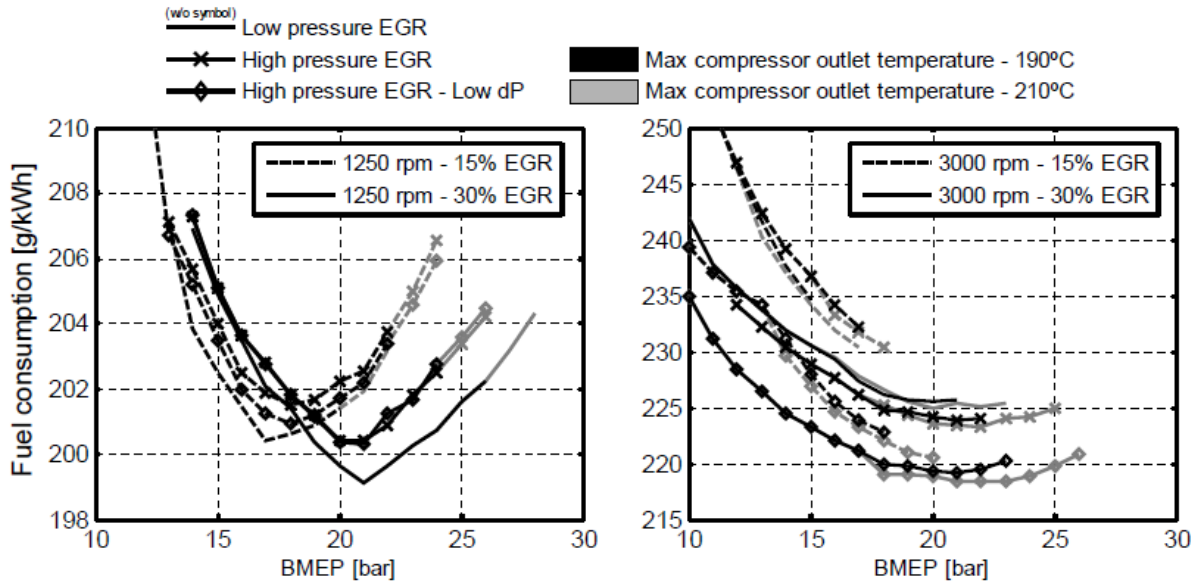


Figure 12: Impact of EGR rates, EGR systems and maximum compressor outlet temperature on engine performance as a function of brake power levels.

327 At 1250 rpm, the different hypotheses assumed on turbocharger efficiencies and element
328 pressure losses forced to use the intake throttle to provide the 15% HP EGR rate. The pressure
329 losses required in the intake line to increase the engine backpressures range from 50 mbar at 15
330 bar BMEP to 300 mbar at 25 bar BMEP. These losses imply higher compression ratios which
331 increase fuel consumption and reduce maximum reachable BMEP by 2 bar. BSFC are thus
332 higher with the HP EGR circuit. At 30% EGR, the intake throttle is no more required due to
333 higher turbocharger works involved. But volumetric efficiency differences still imply higher
334 boost demands for the HP EGR. As the benefits of lower turbocharger gas mass flows do not
335 offset these higher boost demands, the HP EGR circuit stays less efficient. Nonetheless, with its
336 lower compressor inlet temperatures, it allows to reach at this EGR rate 2 bar higher maximum
337 BMEP. Regarding the HP EGR Low dP configuration, no significant differences are noticed at
338 1250 rpm between both HP EGR systems because the elements pressure losses are relatively

339 small at that speed. At 3000 rpm, with identical turbocharger efficiencies and pressure losses,
340 similar fuel consumptions are obtained between both LP and HP circuits. The impacts of dif-
341 ferent volumetric efficiencies are more or less offset by the influences involved by the different
342 turbocharger gas mass flows. Slight benefits can thus be observed for the LP system at 15%
343 EGR while at 30% EGR these benefits are reported for the HP system. However, when the
344 same engine components are used in both circuits, fuel savings of up to 7 g/kWh can be noticed
345 with the HP EGR low dP system. That means the elements pressure drops are the most influen-
346 tial factors when both circuits are compared and pressure losses characteristics are critical for
347 the LP EGR system. Unless large capacity components are employed, the HP circuit presents
348 therefore significant benefits at rated speeds. In terms of maximum BMEP, variations from 1
349 bar to 3 bar give additional advantages to the HP systems. Hypotheses of identical turbocharger
350 efficiencies between both EGR systems are obviously unexpected in practice because the dif-
351 ferent gas mass flows move the running operations to different places in the compressor and
352 turbine maps. At low speeds, turbocharger efficiencies are greater with LP EGR because the
353 higher gas mass flows center the operating conditions in the characteristics maps, while at high
354 speeds this effect is produced with HP EGR. These efficiency variations which strongly depend
355 on the turbocharger maps can therefore positively or negatively influence the results previously
356 found. Nevertheless, these variations are relatively small and generally go in the same direc-
357 tions as the trends observed. Their impacts have thus limited consequences on the obtained
358 conclusions.

359 **4.7 Synthesis of Thermal Constraints with EGR**

360 To synthesize how the EGR rates and thermal constraints limit the engine performance, the
361 maximum reachable BMEP obtained with the different EGR configurations have been plotted
362 in figure 13. With EGR requirements at full load, it can be seen that the maximum allowable

363 compressor outlet temperature is now more restrictive than the maximum allowable exhaust
 364 temperature. In fact, engine performances are limited by compressor outlet temperatures be-
 365 fore exhaust constraints exceed 800°C. As an intermediate intercooler presents limited potential
 366 to reduce the compressor thermal constraints, advanced materials for both compressor wheel
 367 and intake piping are thus necessary for the further development of highly-rated downsized-
 368 downsized engines running at full load with EGR. Titanium compressor impellers able to
 369 withstand higher temperatures and higher cyclical loads are already present in the market for
 370 special applications [103], but their costs are still challenging to see their rapid spread in low to
 371 medium class vehicles.

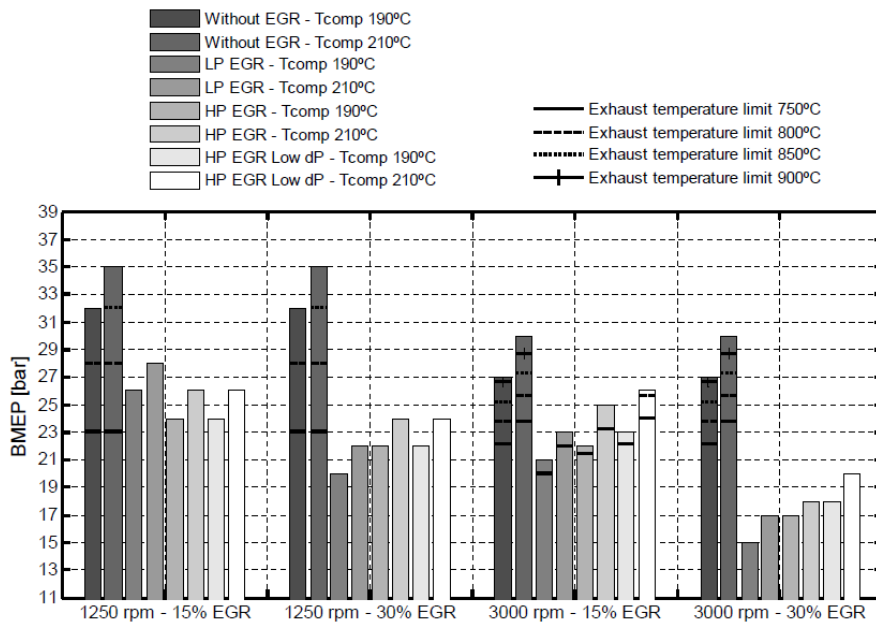


Figure 13: Synthesis of maximum reachable BMEP under LP and HP EGR rates. temperatures

372 5 Two Stage Operation

373 In this subsection, the energetic approach has been extended to the two stage operations. Sim-
 374 ulations have been performed at full load at 1000 rpm and 1250 rpm which represent the most

375 critical two-stage running conditions for the considered boosting architectures. As already men-
376 tioned, the ability of the main turbocharger to produce boost at these speeds is generally very
377 limited and mainly depends on the turbocharger matching. That is why the results have been
378 divided in two representations. On the one hand, the desired boost is entirely provided by the
379 second charger and the engine performances are analyzed as a function of brake power levels.
380 On the other hand, as calculations are not limited by turbocharger operating ranges, the required
381 boost is provided by a combination of both chargers and the engine performances are analyzed
382 as a function of compression ratio distribution for a given brake power level. 0% compression
383 ratio distribution corresponds to a boost demand entirely produced by the main turbocharger
384 while 100% represents one completely supplied by the second charger.

385 Comparing the boosting architectures, a representation is obtained with the different second
386 charger technologies, because the supercharger uses net mechanical power from the crankshaft,
387 the turbocharger recovers waste energy from the exhaust gases and the eBooster consumes
388 electricity supplied by an external source. For the eBooster, the electric consumption is not
389 taken into account in the calculations (free driving energy). It is assumed recovery systems
390 such as regenerative brakes (4) (18) can produce enough electricity to respond to the eBooster
391 demands through energy storages (i.e. supercapacitors). Therefore three electric power levels
392 have been considered for simulations which are 2 kW, 4 kW and 8 kW. To analyze the engine and
393 boosting architecture performance under two stage operations, a first sensitivity study has been
394 performed on the charger efficiencies with the values presented in Figure 3. The calculations
395 have been carried out without EGR, without intermediate intercooler and using the hypotheses
396 of maximum in-cylinder pressures corresponding to future engine developments (see figure 6).
397 These hypotheses have been selected to reduce the influences of in-cylinder pressures limita-
398 tions and to increase the maximum brake power level range for systems comparisons. Since
399 pressure losses characteristics have limited impacts at these speeds, the reference engine com-

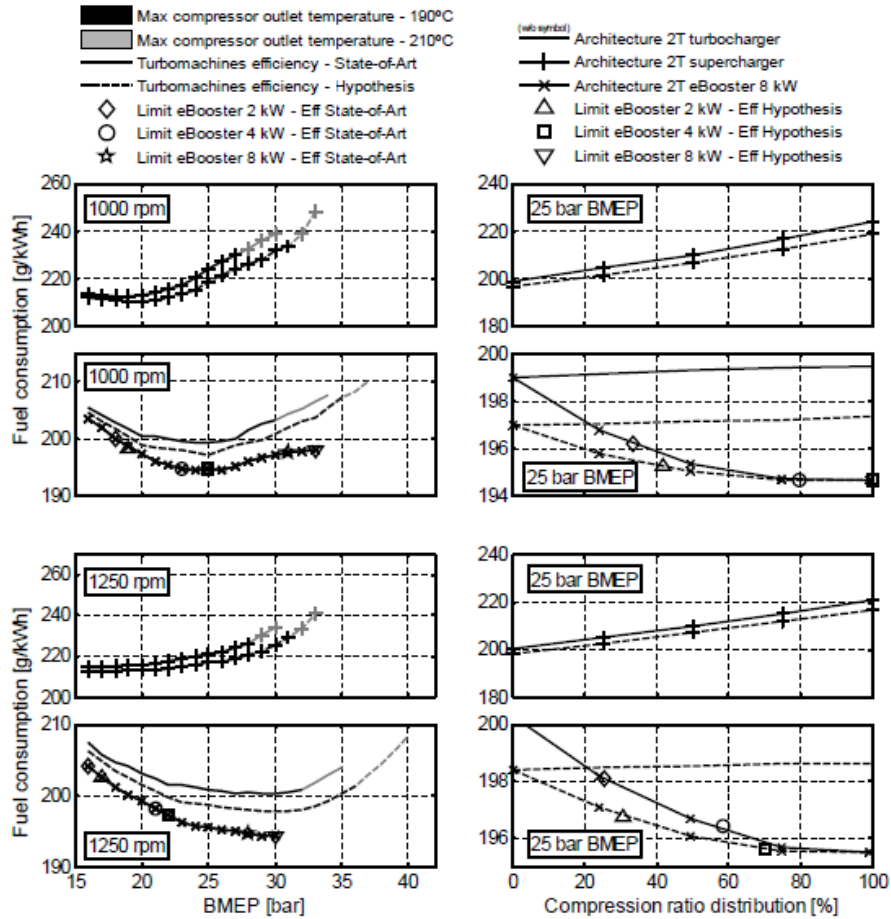


Figure 14: Engine and boosting architecture performance under two-stage operations.

400 ponents described in figure 4 have been retained. The results of this sensitivity study are plotted
 401 in figure 14. As expected, the supercharger presents the highest fuel consumptions. When com-
 402 pared to the turbocharger, the supercharger fuel penalties reach 15 g/kWh at 20 bar BMEP and
 403 more than 35 g/kWh at 35 bar BMEP. Be- tween the turbocharger and eBooster, the differences
 404 are relatively small with values around 5 g/kWh. As the eBooster driving energy has no impact
 405 on fuel consumption, these small differences show the efficiency of the turbocharger to fulfill
 406 the desired boost demands through waste energy recovery from the exhaust gas. Regarding
 407 the efficiency variations, the same conclusions as those obtained in the previous subsection can

408 be noticed for the turbocharger (fuel savings of around 2-3 g/kWh and maximum BMEP in-
409 crease of around 3-4 bar). For the supercharger, an efficiency variation of 10% does not reduce
410 in a significant way the required mechanical power. In fact, BSFC are only decreased from
411 2 g/kWh to 5 g/kWh according to the brake power level. That means efforts in supercharger
412 design optimization do not show important potential to diminish fuel penalties generated by
413 mechanical chargers. The efficiency variation also increases the maximum BMEP by 2-3 bar
414 but, as part of the brake power is employed to drive the supercharger, the maximum BMEP
415 stays around 4-5 bar lower than those reached with the turbocharger. For the eBooster, the
416 maximum reachable BMEP strongly depends on the electric power limitations. For example at
417 1250 rpm with conservative efficiencies, maximum powers of 2 kW, 4 kW and 8 kW restrain
418 the engine performance to 16 bar, 21 bar and 28 bar BMEP respectively. Without these limits,
419 the engine performance could be increased until reaching the maximum allowable compressor
420 outlet temperatures and the corresponding maximum BMEP would be slightly greater than the
421 turbocharger ones. Increasing the eBooster efficiency by 10%, It will reduce the electric power
422 needs allowing for a given electric power level to increase the maximum BMEP by 1-2 bar.
423 The electric power results are shown here for the 2.3l engine. Although BSFC results can be
424 generalized to similar downsized-downspeeded engines, the electric power results rely on gas
425 mass flows and are specific to a given swept volume. They cannot therefore be assumed for
426 other engine displacements. For that reason, the specific power limitations obtained on the 1.2l
427 and 1.6l engine will be presented at the end of this subsection with the synthesis of the max-
428 imum performance results. Thanks to the energetic approach, the impact of the compression
429 ratio distribution between both stages can be analyzed without turbocharger op- erating range
430 limitations. Considering a representative brake power level (25 bar BMEP), it can be seen how
431 the fuel consumption is progressively reduced in the 2T supercharger and 2T turbocharger con-
432 figurations as the proportion of boost provided by the main turbocharger increases. In the 2T

433 eBooster configuration, this trend is reversed as the electric power is supplied by an external
434 source. At this brake power level, modifying the compression ratio distribution from 100% to
435 0% brings for the 2T supercharger configuration fuel benefits of up to 20 g/kWh. This is mainly
436 explained by the reduction of brake power needs. For the 2T turbocharger configuration, these
437 fuel benefits are much smaller reaching only 2 g/kWh due to the limited efficiencies differ-
438 ences between both turbochargers. These small fuel savings give thus certain flexibility to the
439 boosting architecture to optimize other objectives such as engine control, mode transition,
440 EGR abilities at part loads [345], etc. . . without significantly deteriorating the fuel consump-
441 tion. For the 2T eBooster configuration, using the main turbocharger can increase the BSFC
442 up to 3-4 g/kWh. However in this architecture the selection of the optimum compression ratio
443 distribution depends not only on the main turbocharger boost abilities but also on the electric
444 power limitations which can make unachievable a 100% distribution. For example here with
445 conservative efficiencies, the 2 kW and 4 kW maximum electric powers limit the compression
446 ratio distribution at 25% and 58% respectively.

447 **5.1 Effect of Interstage Cooling**

448 With the same approach, the fuel benefits obtained using an intermediate intercooler have also
449 been analyzed for two brake power levels (20 bar and 30 bar BMEP). With this cooler, the
450 maximum reachable BMEP have not been considered due to the extremely high values that
451 could theoretically be achieved. After a first compression in the LP stage, an intermediate
452 intercooler allows to reduce the HP compression work increasing the gas density at the HP
453 charger inlet. Nonetheless, adding an intermediate intercooler increases the pressure losses
454 in the intake line. Fuel savings are thus a balance between both effects. The intermediate
455 intercooler operates only at low speeds during two-stage operations. Its design is generally
456 smaller than that of the after-cooler. However here to analyze an optimistic situation, the same

457 pressure losses characteristics have been retain in both coolers.

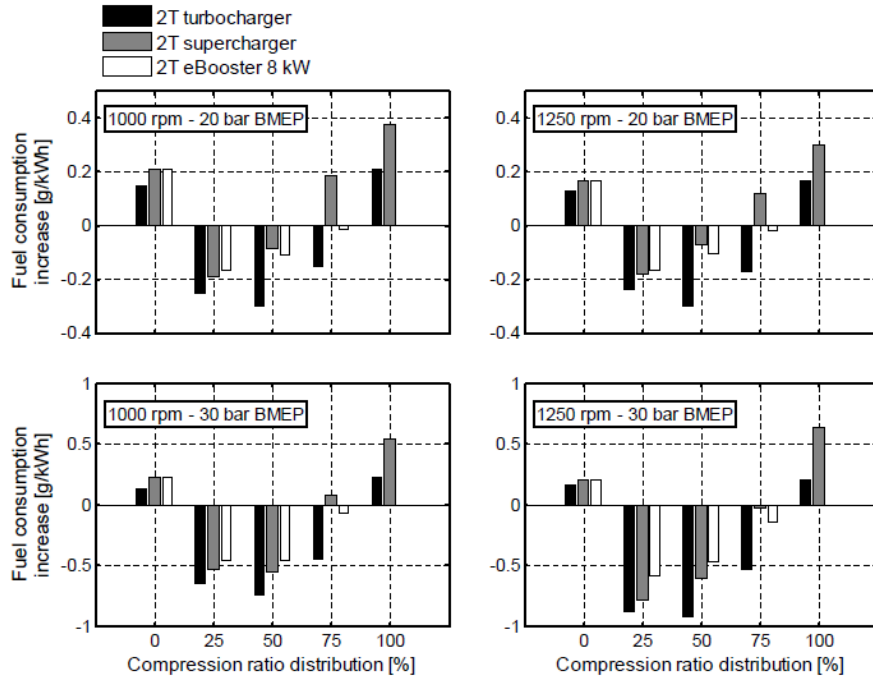


Figure 15: Impact of inter-stage cooling on engine fuel consumption as a function of compression ratio distribution.

458 The results of this study are shown in figure 15 as a function of compression ratio distribu-
 459 tion. At 0% and 100% compression ratio distribution, there is obviously no fuel benefit from
 460 compression work reductions and the results reflect fuel penalties generated by higher pressure
 461 losses. The differences observed at 0% between the different architectures mainly lie in the in-
 462 tercooler relative position. In fact in the 2T turbocharger configuration, the intercooler is fitted
 463 downstream the main turbocharger while in the 2T supercharger and 2T eBooster configura-
 464 tions it is placed upstream. At 100%, the differences are higher with the supercharger as the
 465 pressure losses must be offset using mechanical power, while they are null with the eBooster as
 466 its electric consumption is not considered. For the 2T configuration, at 25% the HP compres-
 467 sion work is relatively small. So, a reduction of this work has limited consequences on the fuel
 468 consumption. At 75%, the HP charger work is much more important but the temperature rise

469 in the LP charger is relatively small. So, an intermediate cooling process has also little effect
470 and the maximum benefits are obtained around 50%. For the other configurations, the same ef-
471 fects are noticed but the maximum benefits are rather observed around 75% due to the different
472 costs that represent offsetting the pressure losses with the second charger (any impact with the
473 eBooster while important fuel penalties with the supercharger). At the end, the fuel benefits
474 are generally very small with maximum values of around 0.2 g/kWh at 20 bar BMEP and 0.9
475 g/kWh at 30 bar BMEP. So, even though the main turbocharger has the ability to produce boost
476 at low speeds, these small fuel savings do not justify the cost and packaging constraints that
477 involve the implementation of an intermediate intercooler.

478 **5.2 Effect of EGR Level in 2-Turbo Operation**

479 To complete the results obtained under two-stage operations, a second sensitivity study has
480 been performed on EGR rates provided by the LP EGR circuit (0%, 15% and 30%). Here the
481 HP circuit has not been considered because, on the one hand, the supercharger and eBooster
482 do not have any ability to produce the required engine backpressures, and on the other hand
483 the main conclusions regarding the differences between HP and LP systems working with a
484 turbocharging architecture have already been given in the last subsection.

485 The calculations have been carried out with conservative efficiencies and without intermedi-
486 ate intercooler. The results are plotted in figure 16 using the representations previously defined.

487 With the hypotheses assumed on the elements pressure losses characteristics, LP EGR has
488 an impact on the combustion process and chargers work. For the e-Booster, the compressor
489 work is produced with electricity coming from an external source. The fuel benefits of around
490 5 g/kWh that can be observed between the different EGR rates correspond therefore to the
491 combustion efficiency improvements generated by the injection timings strategy. For the tur-
492 bocharger, the higher compression works increase the turbine expansion ratios and the resultant

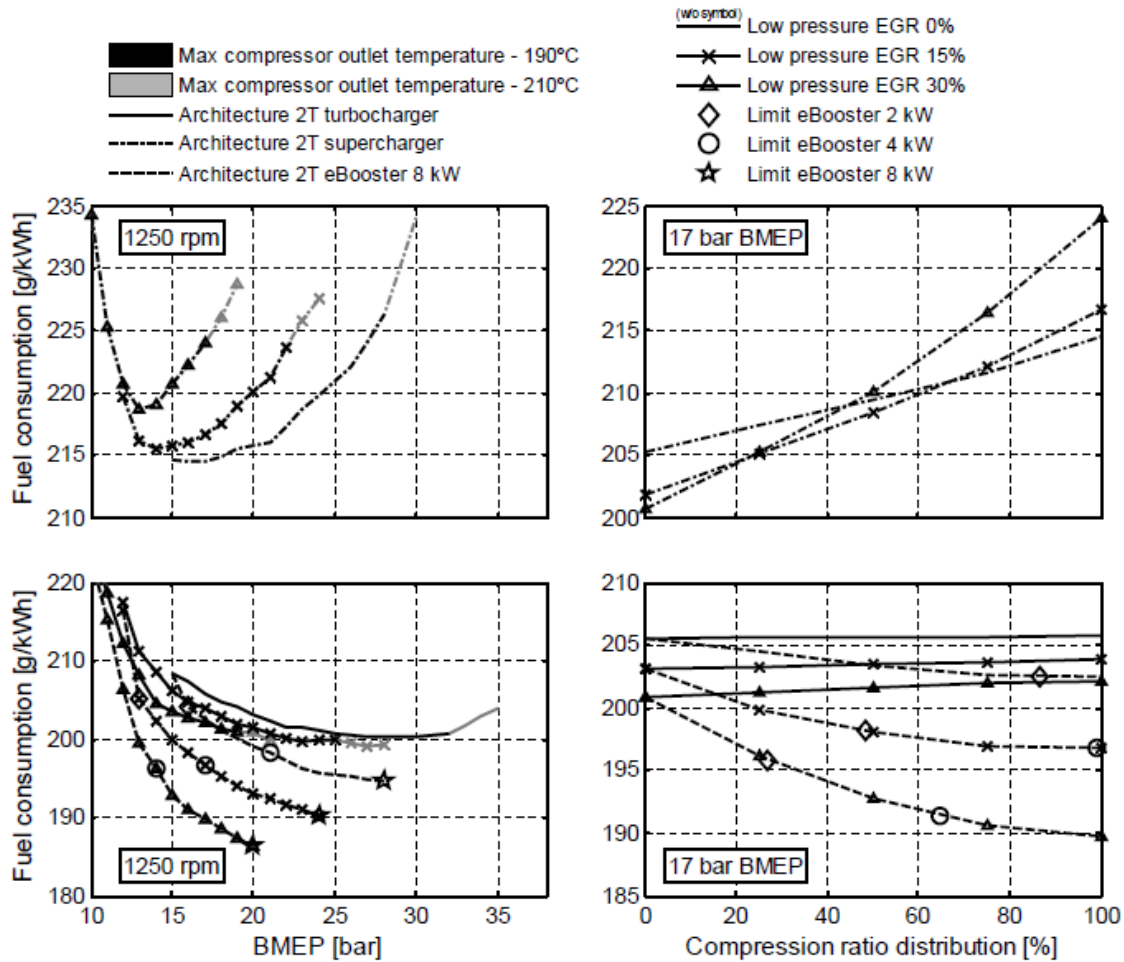


Figure 16: Impact of LP EGR rates, electrical power limitations and maximum compressor outlet temperature on engine and boosting architecture performance under two-stage operations.

493 engine backpressure losses. Comparing the e-Booster and turbocharger results, the fuel penal-
 494 ties involved by these losses can thus be estimated to around 8 g/kWh and 13 g/kWh at 15% and
 495 30% LP EGR respectively. However here, the combustion improvements offset these loses and
 496 BSFCs are maintained almost constant between the different EGR rates. For the supercharger,
 497 the fuel penalties involved by higher brake power demands are too important to be offset by
 498 the combustion improvements and fuel consumptions are deteriorated under LP EGR. In terms
 499 of maximum engine performance, increasing by 15% the LP EGR rate reduces the maximum

500 BMEP by 5-7 bar in the case of the turbocharger and supercharger due to the maximum com-
501 pressor outlet temperatures, while this reduction is around 2-4 bar with the e-Booster due to
502 limited electric power levels. Regarding the compression ratio distribution influences, it can
503 be noticed the same trends as those previously described for the two-stage operations running
504 without EGR.

505 **5.3 Synthesis of Thermal Constraints in 2 Turbo Operations**

506 Finally, to synthesize how the thermal constraints, the EGR rates and the electric power levels
507 limit the engine performance, the maximum reach- able BMEP obtained under two-stage op-
508 erations have been plotted in figure 17. As it can be observed, when the electric power is not
509 restrained, the 2T e-Booster architecture allows to reach 1-2 bar higher maximum BMEP than
510 the 2T turbocharger configuration due to free exhaust gas mass flows. Whereas, the 2T super-
511 charger architecture reaches 2-5 bar lower maximum BMEP due to brake power consumption.
512 For the thermal constraints, if the exhaust temperature limitations are lower than 850°C, the
513 maximum exhaust temperature stays the limiting factor in the 2T turbocharger configuration
514 running without EGR. Otherwise, with higher exhaust temperature limitations or under EGR,
515 the maximum compressor outlet temperature becomes more restrictive. In the 2T e-Booster and
516 2T supercharger configurations, the exhaust temperature limitations are not so critical because
517 the engine backpressures are significantly lower. In these architectures, the maximum compres-
518 sor outlet temperature is therefore always the limiting factor. Modifying the thermal resistance
519 of the intake piping system from 190°C to 210°C presents thus important benefits in most cases
520 to improve by 2-3 bar the maximum reachable BMEP.

521 Regarding the electric constraints, the electric power level requirements are proportional to
522 the gas mass flows which mainly depend on the engine displacement. Here, it can be noticed
523 how the 2 kW, 4 kW and 8 kW electric power limitations restrain the maximum reachable

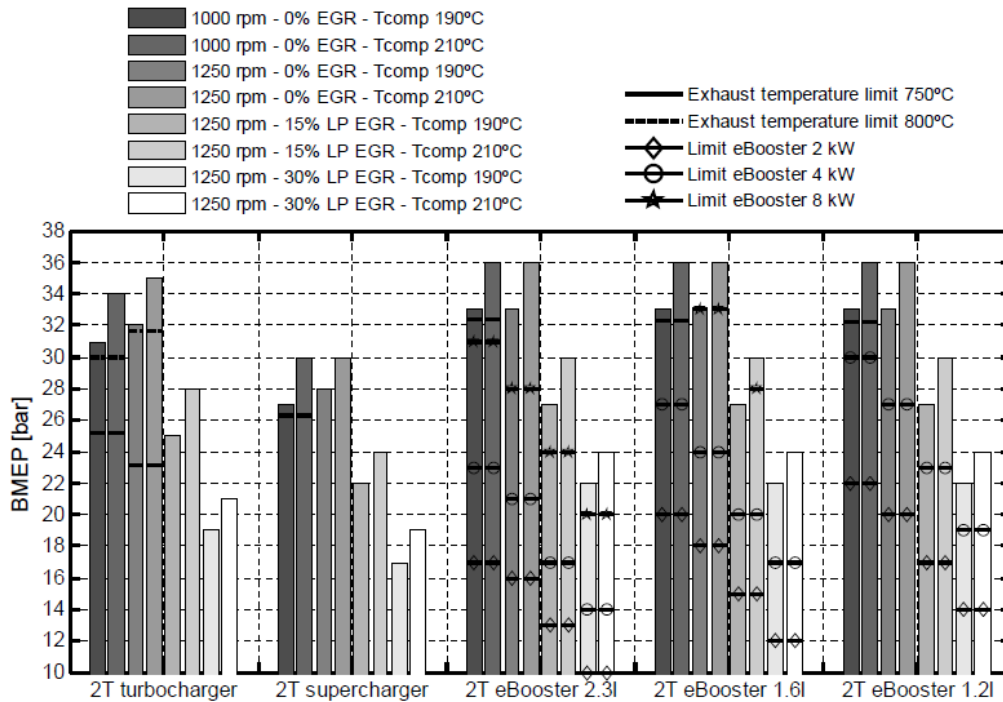


Figure 17: Synthesis of maximum reachable BMEP in two-stage operation.

524 BMEP for the different engine displacements. To achieve the maximum compressor outlet
 525 temperatures, the electric power levels must approximately exceed 10 kW, 8 kW and 6 kW for
 526 the 2.3l, 1.6l and 1.2l engines respectively. The maximum electric power level defined by the
 527 e-Booster motor or by the electric vehicle network is therefore in most cases the limiting factor
 528 to reach high low-end torques with the 2 Turbo e-Booster configuration.

529 6 Conclusion

530 According to the parametric study to characterize the limits and performance of the most
 531 promising boosting architecture on the base engines. Simulations have been performed with
 532 the 0D engine model and a specific methodology has been defined to obtain general conclu-
 533 sions valid for most downsized-downspeeded engines. This methodology is based on the sim-

534 ilarity theory to reproduce analogous behavior between the different downsized engines and,
535 for the steady-state calculations, it is also based on an energetic approach to avoid influences
536 of specific components designs (hypotheses on intake/exhaust line element characteristics, tur-
537 bocharger maps, etc. . .). Several sensibilities studies have been conducted to determine
538 the main factors that govern the architecture performance and to quantify their impacts on
539 fuel consumption and maximum rated power. These factors regroup the parameters such as
540 turbocharger efficiencies, engine elements pressure losses characteristics, thermomechanical
541 limitations (maximum in-cylinder pressure, exhaust manifold temperature, compressor outlet
542 temperature, etc. . .), EGR rates and EGR system technology (HP and LP circuits). In two-
543 stage operations, additional analyses have also been performed to compare the performance
544 of the considered architectures characterizing the different systems interactions and evaluating
545 possible interstage cooling benefits. From these results, the required charger operating ranges
546 have been confronted to conservative characteristics maps. Through a representative data base
547 that allows the actual technological limits to be judged, new requirements have been defined
548 for future turbocharger developments and new characteristic maps have been extrapolated to
549 perform transient calculations.

550 **References and Notes**

- 551 1. J Arrègle, JJ López, JM Garcia, and C Fenollosa. Development of a zero-dimensional
552 diesel combustion model. part 1: analysis of the quasi-steady diffusion combustion phase.
553 *Applied Thermal Engineering*, 23(11):1301–1317, 2003.
- 554 2. Carlo Beatrice, Giovanni Avolio, Nicola Del Giacomo, and Chiara Guido. Compression
555 ratio influence on the performance of an advanced single-cylinder diesel engine operating
556 in conventional and low temperature combustion mode. Technical report, SAE Technical
557 Paper, 2008.
- 558 3. Alberto A Boretti and Giuseppe Cantore. Similarity rules and parametric design of race
559 engines. Technical report, SAE Technical Paper, 2000.
- 560 4. Enrico Cacciatori, Baptiste Bonnet, Nicholas D Vaughan, Matthew Burke, David Price, and
561 Krzysztof Wejrzanowski. Regenerative braking strategies for a parallel hybrid powertrain
562 with torque controlled ivt. Technical report, SAE Technical Paper, 2005.
- 563 5. G Cantore and E Mattarelli. Similarity rules and parametric design of four stroke motogp
564 engines. Technical report, SAE Technical Paper, 2004.
- 565 6. A Chasse, P Moulin, P Gautier, A Albrecht, L Fontvieille, A Guinois, and L Doléac. Double
566 stage turbocharger control strategies development. *SAE International Journal of Engines*,
567 1(2008-01-0988):636–646, 2008.
- 568 7. G Cipolla, A Vassallo, AE Catania, Ezio Spessa, C Stan, and L Drischmann. Combined
569 application of cfd modeling and pressure-based combustion diagnostics for the develop-
570 ment of a low compression ratio high-performance diesel engine. Technical report, SAE
571 Technical Paper, 2007.

- 572 8. J Galindo, JR Serrano, C Guardiola, and C Cervelló. Surge limit definition in a specific
573 test bench for the characterization of automotive turbochargers. *Experimental Thermal and*
574 *Fluid Science*, 30(5):449–462, 2006.
- 575 9. José Galindo, A Tiseira, FJ Arnau, and R Lang. On-engine measurement of turbocharger
576 surge limit. *Experimental Techniques*, 37(1):47–54, 2013.
- 577 10. Francisco Payri González and José M^a Desantes Fernández. *Motores de combustión interna*
578 *alternativos*. Editorial Universitat Politècnica de València, 2011.
- 579 11. Hermann Hiereth and Peter Prenninger. *Charging the internal combustion engine*. Springer
580 Science & Business Media, 2007.
- 581 12. P Hoecker, JW Jaisle, and S Munz. The ebooster from borgwarner turbo systems-the key
582 component for a new automobile charging system. *Borg Warner Turbo Systems Knowledge*
583 *Library*, page 5, 2000.
- 584 13. N.Ausserhofer M.Weissbaeck O.Soustelle P.Ragot P. Mallet M.F.Howlett, W.Schnider and
585 J. Rozen. 3 cylinder aggressive downsized diesel. 2010.
- 586 14. S Münz, M Schier, HP Schmalzl, and T Bertolini. ebooster design and performance of a
587 innovative electrically driven charging system, 2008.
- 588 15. Alexandros Plianos and Richard Stobart. Modeling and control of diesel engines equipped
589 with a two-stage turbo-system. Technical report, SAE Technical Paper, 2008.
- 590 16. José Ricardo Hector, Galindo Lucas. *Contribución a la Mejora del Margen de Bombeo en*
591 *Compresores Centrífugos de Sobrealimentación*. PhD thesis, 2011.
- 592 17. JR Serrano, FJ Arnau, V Dolz, A Tiseira, M Lejeune, and N Auffret. Analysis of the
593 capabilities of a two-stage turbocharging system to fulfil the us2007 anti-pollution directive

- 594 for heavy duty diesel engines. *International Journal of Automotive Technology*, 9(3):277–
595 288, 2008.
- 596 18. Gino Sovran. The impact of regenerative braking on the powertrain-delivered energy re-
597 quired for vehicle propulsion. Technical report, SAE Technical Paper, 2011.
- 598 19. Richard Van Basshuysen and Fred Schäfer. *Internal combustion engine handbook-basics,*
599 *components, systems and perspectives*, volume 345. 2004.
- 600 20. G. Oberholz V.Simon and M. Mayer. *The Impact of Regenerative Braking on the*
601 *Powertrain-Delivered Energy Required for Vehicle Propulsion*. Bog Warner Turbo Sys-
602 tem Knowledge Library, 2000.
- 603 21. Neil Watson and Marian Stefan Janota. *Turbocharging: The internal combustion engine*.
604 MacMillan, 1982.